Intestinal damage in enterohemorrhagic Escherichia coli infection.

Békassy, Zivile; Calderon Toledo, Carla; Leoj, Gustav; Kristoffersson, Ann-Charlotte; Leopold, Shana R; Perez, Maria Thereza; Karpman, Diana

Published in:
Pediatric Nephrology

DOI:
10.1007/s00467-010-1616-9

2011

Intestinal damage in enterohemorrhagic *Escherichia coli* infection

Zivile D. Békássy[1], Carla Calderon Toledo[1], Gustav Leoj[1], AnnCharlotte Kristoffersson[1], Shana R. Leopold[2], Maria-Thereza Perez[3], Diana Karpman[1*]

[1]Department of Pediatrics and [3]Department of Ophthalmology, Clinical Sciences Lund, Lund University, Lund Sweden. [2]Department of Pediatrics, Washington University School of Medicine, St Louis MO

Keywords: Enterohemorrhagic *Escherichia coli*, Shiga toxin, intimin, *E. coli* secreted proteins, type III secretion system

* Corresponding author:
Diana Karpman
Department of Pediatrics
Lund University
22185 Lund
SWEDEN
e-mail: Diana.Karpman@med.lu.se
Telephone: + 46 46 2220747 / fax: + 46 46 2220748

This study was supported by grants from The Swedish Research Council (K2010-65X-14008 to DK and 12209 to MTP), Torsten and Ragnar Söderberg Foundation, The Fund for Renal Research, Crown Princess Lovisa's Society for Child Care, Konung Gustaf V:s 80-årsfond, Fanny Ekdahl's Foundation (all to DK). National Institutes of Health Grant 5P30 DK052574 (to Washington University Digestive Diseases Research Core Center), National Institutes of Health Grant 5T32AI007172 and R56AI063282 (in support of SRL). Diana Karpman is the recipient of a clinical-experimental research fellowship from the Royal Swedish Academy of Sciences.

Abstract

Enterohemorrhagic *Escherichia coli* infection leads to marked intestinal injury. Sigmoid colon obtained from two children during EHEC infection exhibited abundant TUNEL-positive cells. To define which bacterial virulence factors contribute to intestinal injury the presence of Shiga toxin-2 (Stx2), intimin and the type III secretion system were correlated to symptoms and intestinal damage. C3H/HeN mice were inoculated with Stx2-producing (86-24) and non-producing (87-23) *E. coli* O157:H7 strains and 86-24 mutants lacking *eae*, encoding intimin, (strain UMD619) or *escN* regulating the expression of type III secretion effectors (strain CVD451). Severe symptoms developed in mice inoculated with 86-24 and 87-23. Few mice inoculated with the mutant strains developed severe symptoms. Strain 86-24 exhibited higher fecal bacterial counts, followed by 87-23, whereas strains UMD619 and CVD451 showed minimal fecal counts. More TUNEL-positive cells were found in proximal and distal colons of mice inoculated with strain 86-24 compared to strains 87-23 and CVD451 ($p \leq 0.01$) or UMD619 ($p < 0.05$, proximal colon, $p < 0.01$, distal colon). The results show that strains 86-24 and 87-23 exhibited better colonic persistence and more symptoms, presumably due to the presence of intimin and type III secretion effectors. Extensive intestinal mucosal cell death was related to the presence of Stx2.

Introduction

EHEC infection is associated with gastroenteritis manifesting as non-bloody or bloody diarrhea, and in severe cases the development of hemolytic uremic syndrome (HUS) [1]. Intestinal damage usually leads to hemorrhagic colitis. Macroscopic and microscopic changes have been evaluated in intestinal samples obtained from patients with severe symptoms who underwent hemicolectomy, biopsy or autopsy and may reflect the most extreme cases of intestinal involvement. Pathological lesions consisted of edema, hyperemia and hemorrhage, fibrinous exudates, vascular thrombosis, mucosal necrosis and pseudomembrane formation [2].

Animal models of EHEC infection have demonstrated gastrointestinal symptoms, such as diarrhea, and pathology in calves, gnotobiotic piglets, rabbits and mice [3-8]. Inflammatory colitis as well as necrotizing enterocolitis were shown in infected gnotobiotic piglets [4] and rabbits [5]. Colons from infected mice exhibited bleeding, edema and erosions, congestion of the lamina propria with thickening of the submucosa, inflammation, damaged crypts, goblet cell depletion and necrosis [6-8].

Although the colon is the main part of the gastrointestinal tract affected during EHEC infection, the initial colonization occurs in the ileum. Using in vitro intestinal organ cultures EHEC serotype O157:H7 was found to initially colonize the villi of the distal ileum and follicle-associated epithelium of Peyer's patches [9, 10]. This is presumably followed by colonization of the colon [10]. EHEC establish attaching and effacing (A/E) lesions on the intestinal mucosa characterized by effacement of intestinal microvilli and intimate attachment to the epithelial cell. Actin polymerization in enterocytes leads to the formation of a pedestal onto which the bacteria adhere (reviewed in Nataro and Kaper [11]). This form of adherence

is mediated by intimin, an outer membrane protein encoded by the *eae* gene [12, 13], by *E. coli* secreted proteins (Esps) A, B and D secreted by a type III secretion system (T3SS) [11], by Tir (translocated intimin receptor) and the Tir-cytoskeleton coupling protein TccP [14], also termed $EspF_U$, as well as by the *esc* and *sep* genes [13]. The genes for all these factors are located on a bacterial chromosomal pathogenicity island called the LEE (locus of enterocyte effacement) [12]. EspA forms a filament via which EspB and Tir are translocated into the intestinal epithelial cell whereas EspB and EspD may form a pore in the host cell membrane through which bacterial proteins are injected into the cell [15].

The severity of EHEC infection is attributed to Shiga toxin (Stx) [16]. Stx binds to the globotriaosylceramide (Gb3) receptor on intestinal Paneth cells [17] but not to the intestinal epithelium as these cells lack Gb3. All the same Stx induces an intestinal inflammatory response [18] and translocates across the intestinal epithelial barrier [19]. Stx may induce apoptosis of rabbit intestinal epithelial cells *in vivo* [20] and human intestinal cells in vitro [21].

We have previously described a mouse model of *E. coli* O157:H7 infection [6] in which mice developed gastrointestinal, neurological and systemic symptoms with histopathology of the intestines and kidneys. These mice were not streptomycin-treated so as not to diminish the commensal microflora. The aim of the present study was to investigate the presence of colonic cell death due to EHEC in human and murine infection and to correlate the expression and secretion of *E. coli* O157:H7 factors to the development of symptoms and intestinal injury using wild-type Stx-2 producing and non-producing *E. coli* O157:H7 and mutants that do not express intimin or secrete Tir, Esps A, B and D.

Material and methods

Intestinal tissue from patients and controls

Sigmoid colon tissue was available from two children treated at the Department of Pediatrics, Lund University Hospital for EHEC-associated hemolytic uremic syndrome (HUS). Partial sigmoidectomy was carried out in both cases due to colonic perforation. One pediatric control underwent resection of a larger part of the sigmoid colon and two pediatric controls underwent colonic biopsy. These children did not have a history of hemorrhagic colitis or HUS and their tissue samples were deemed normal by the hospital pathologist. The patients as well as pediatric controls are described in Table 1. Tissue samples from patients and controls were obtained with informed written parental consent and the study was approved by the Ethics Committee of the Medical Faculty at Lund University. The biopsy material obtained was transferred into physiologic NaCl solution for approximately 30 min followed by paraformaldehyde fixation, according to hospital routines, while all surgically resected tissue was directly paraformaldehyde-fixed in the operating room. Colonic tissue was stained with hematoxylin-eosin or periodic acid Schiff and assessed by light microscopy. CD14 was detected in the human tissues by immunohistochemistry. using a previously described method [22], for details see the supplementary data (SD). Colonic tissue was also assessed by fluorescence microscopy using the terminal deoxynucleotidyl transferase (TdT)-mediated dUPT-biotin nick-end-labelling (TUNEL) assay as described below.

Mice

C3H/HeN mice were bred in the animal facilities at the Department of Microbiology, Immunology and Glycobiology, Institute of Laboratory Medicine, Lund University. Female and male mice were used at 8-16 weeks of age. The study was approved by the animal ethics committee of Lund University (protocol no. M 231-05).

Bacteria

The bacterial strains used in this study are listed in Table S1 (see the SD). The *E. coli* O157:H7 strains, 86-24 (Stx2-producing) and 87-23 (Stx non-producing) were isolated during the Walla Walla outbreak of hemorrhagic colitis and HUS in 1986 [23] and were kindly provided by A.D. O'Brien (Department of Microbiology and Immunology, Uniformed Services University of the Health Sciences, Bethseda, MD, USA). These strains were previously characterized regarding serotype, plasmid content, enterohemolysin, the presence of *stx* and *eae* genes, enterohemorrhagic *E. coli* 60-MDa plasmid, enteroaggregative *E. coli* localized adherence probe, enteropathogenic *E. coli* adherence factor, diffuse adherence *E. coli* probe and the Vero cell assay [6]. The strains differed only in the production of Stx2 and cytotoxicity for Vero cells [6]. The isogenicity of strains 86-24 and 87-23 was determined (see SD for methodology and Table S2). The presence of the O157 serogroup antigen was confirmed by slide agglutination using an *E. coli* O157 latex test kit (Oxoid, Basingstoke, UK).

Two mutant strains based on the parental 86-24 strain were used, UMD619 with a deletion in the *eae* gene encoding intimin and CVD451 with an insertion mutation affecting the *escN* gene required for secretion of Tir and *E. coli* secreted proteins A, B and D. As controls, these bacteria with plasmids complemented with the respective genes were used ($UMD619_{pCVD444}$ and $CVD451_{pCVD446}$). The UMD619, CVD451, $UMD619_{pCVD444}$ and $CVD451_{pCVD446}$ strains were kindly provided by J.B. Kaper (Center for Vaccine Development, University of Maryland, Baltimore, MD, USA). *E. coli* FN414 was selected as a fecal control strain since it lacked genotypic and phenotypic traits associated with Stx-producing *E. coli* [6]. Stock cultures of all strains were maintained in Luria-Bertani broth/glycerol (85/15% v/v) at -80°C

until used. Strains were subcultured on Tryptic Soy Agar plates using appropriate antibiotics (see Table S1 in the SD) at the following concentrations: tetracycline 12 µg/ml, ampicillin 50 µg/ml and kanamycin 30 µg/ml. Before inoculation, the strains were grown in Luria broth overnight with appropriate antibiotics, harvested by centrifugation, washed twice in sterile phosphate-buffered saline (PBS pH 7.4; Medicago AB, Uppsala Sweden) and resuspended in PBS at a concentration of 10^9 cfu/ml.

In order to enhance the virulence mice were first inoculated intragastrically with each parental strain. Colons and feces were cultured when the mice developed obvious symptoms (as described below) 2-3 days post-inoculation. Cultures obtained from the colons of sick mice inoculated with *E. coli* O157:H7 strains 86-24, 87-23, $UMD619_{pCVD444}$ or $CVD451_{pCVD446}$ were termed "INT" (standing for intestine) as listed in Table S3 in the SD. Colonic cultures of the mice inoculated with UMD619 and CVD451 were negative. A fecal UMD619 strain was isolated from one sick mouse and termed "UMD619FE" (FE standing for feces). Mice inoculated with CVD451 did not develop symptoms during these initial experiments and the parental strain was therefore used in all experiments. The FN414 strain has previously been shown to be avirulent in this mouse model [6] and was therefore not passaged through mice. The parental strain was used.

Infection protocol

Mice were fasted for food but not for water for 20-24 h before inoculation. Under isoflurane anaesthesia (Forene Abbot, Wiesbaden, Germany) 100 µL bacterial suspension at 10^9 cfu/mL in PBS was deposited intragastrically through a soft polyethylene catheter (outer diameter, 0,61 mm; Clay Adams, Parsippany, NJ, USA) [6]. The controls received 100 µL sterile PBS. After inoculation the catheter was removed, food was reintroduced and provided ad libitum.

Mice were monitored at least every 8 hours and a symptom score from 0 (no symptoms) to 4 (death) was given to each mouse as presented in Table S4 in the SD. Mice were particularly examined for gastrointestinal (changes in fecal color and consistency), neurologic (defined as severe symptoms and including ataxia, rigidity, spasticity, convulsions, coma), and/or systemic symptoms (ruffled fur, hunched back, reduced response upon stimulation, tremor or shivering, lethargy). After five days or when evident signs of disease were observed, inoculated and control mice were sacrificed by cervical dislocation.

Fecal cultures and bacterial burden

Fecal cultures were collected from mice 24 h and 96 h after inoculation and cultured on TSA plates without antibiotics (for strains 86-24INT and 87-23INT) and with appropriate antibiotics for strains UMD619FE, UMD619$_{pCVD444}$INT, CVD451 and CVD451$_{pCVD446}$INT. *E. coli* 0157 serotype was identified by the latex agglutination test.

As not all strains used carried antibiotic resistance, bacterial burden was carried out by colony hybridization. For a detailed description see the SD.

Histopathological analysis

Following assessment for gross pathological changes, colonic tissue was processed for histopathological analysis. Proximal and distal colons of mice were fixed for 24 hours in 4% paraformaldehyde (Sigma-Aldrich, St. Louis, MO, USA) embedded in paraffin, sectioned (3 µm), stained with periodic acid Schiff and examined by light microscopy. To quantify inflammatory infiltrates clusters of six or more inflammatory cells were counted in the colonic tissues.

TUNEL assay

The TUNEL method was used to identify dying cells following a previously described protocol [24, 25]. For a detailed description see the SD. TUNEL positive cells were visualized using a fluoresence microscope Nikon ECLIPSE ε 800 (Nikon, City, Japan) mounted with an Olympus DP70 camera. The software AnalySIS Image Processing, version 3.2 (Olympus Soft Imaging System GmbH, Münster, Germany) was used for quantitating labelled cells in colonic tissue within an area of 1-11 mm^2. Values were normalized and expressed as the number of TUNEL-positive cells per 100 000 μm^2 of colonic tissue.

Caspase- 3 assay

The presence of activated caspase-3, as a marker of apoptosis, was investigated in mouse intestines by immunohistochemistry using SignalStain Cleaved Caspase-3 (Asp 175) IHC Detection Kit (Cell Signaling Technology, Danvers MA, USA) as per the manufacturer's instructions.

Statistical Analysis

Statistical comparison of the effects of virulence factors on symptoms in mice inoculated with the different strains and PBS controls were evaluated by the Fisher's exact test. Comparison of the number of inflammatory clusters and the number of TUNEL-positive cells in intestinal tissue of the different groups of mice was evaluated with the Mann-Whitney test. The SPSS program (version 15.0, Chicago, Ill, USA) was used. $P < 0.05$ was considered significant.

Results

EHEC infection leads to severe histopathological changes in the human sigmoid

Sigmoidectomy was performed in two patients with HUS. A thickened and necrotic area of the sigmoid colon was removed from Patient 1 exhibiting a transmural perforation. There was a deep ulceration in the adjacent tissue involving the muscularis propria and subserosa. Areas of inflammatory infiltrates and hemorrhages were visible by light microscopy as shown in Figure 1a. The sigmoid colon was removed from Patient 2 due to a central perforation covered with fibrin exudates. Total necrosis extended throughout the entire mural wall (Figure 1b). At the resection borders focal necrotic areas were seen with granulation tissue penetrating the muscularis propria. The tissue was hyperemic with massive inflammatory infiltrates. For comparison normal colonic mucosa from pediatric controls was examined as shown in Figure 1d.

TUNEL-positive cells in the human sigmoid during EHEC infection

Abundant TUNEL-positive nuclei were demonstrated in the lamina propria in the mucosa of the sigmoideum removed from both HUS patients (Figures 1e and 1g show tissue from Patient 1, see Figures 1f and 1h for adjacent hematoxylin-eosin stained sections). TUNEL positive cells were found in all layers of the sigmoid section. The labelled areas included intestinal cells, vascular cells as well as inflammatory cells. CD14-positive cells were found in the submucosa of sigmoid colon from Patient 1 in the same area in which multiple TUNEL-positive cells were visualized indicating the presence of macrophages and/or monocytes in these regions (Figure S1 in the SD). Few TUNEL-positive nuclei were noted in the colon from control tissues (Figure 1c). CD14-positive cells were not demonstrated in the colon from Control 2 (data not shown).

The results indicate that affected areas of the sigmoid colon removed from patients with EHEC infection contain multiple TUNEL positive cells. We therefore continued to examine which EHEC virulence factors contributed to symptoms, intestinal damage and intestinal cell death in a mouse model.

Shiga toxin, intimin, Tir and *E. coli* secreted proteins promote disease in mice

C3H/HeN mice (n=115) were intragastrically inoculated with *E. coli* O157:H7 strains 86-24INT, 87-23INT, UMD619FE, UMD619$_{pCVD444}$INT, CVD451, CVD451$_{pCVD446}$INT, as well as the non-virulent strain *E. coli* strain FN414. Mice were observed for gastrointestinal, neurologic and systemic symptoms and signs of clinical disease were compared between mice inoculated with the various strains and PBS controls (Figure 2). Most mice that developed symptoms demonstrated initial signs of disease within the first 24 hours (Table 2). Mice that developed severe symptoms and death (symptom scores 3-4) presented with ruffled fur, hunched posture and decreased activity followed in certain mice by neurological symptoms such as ataxia and rigidity within two to three days after challenge. Mice that developed milder symptoms (symptom scores 1-2) and were not sacrificed recovered spontaneously within the observation period of five days. The most severe symptoms developed in mice inoculated with the wild-type Stx-producing 86-24INT strain in which 20/25 mice developed symptoms and 11 of the mice developed severe symptoms including neurological symptoms. The wild-type Stx-negative strain 87-23INT also led to severe systemic symptoms in 6/20 mice. No neurological symptoms were observed in the latter group.

Ten of 25 mice inoculated with strain UMD619FE developed symptoms of which 8 developed mild symptoms and recovered. Six of 10 mice inoculated with UMD619$_{pCVD444}$INT

developed symptoms, of which severe symptoms developed in 3/10 mice resembling symptoms in mice inoculated with the 86-24INT strain, as expected.

None of 23 mice inoculated with strain CVD451 developed severe symptoms and only 7/23 developed milder systemic symptoms and recovered by day 3 post-inoculation. Five of 10 mice inoculated with strain CVD451$_{pCVD446}$INT strain developed symptoms of which two mice exhibited severe symptoms, comparable to those in mice inoculated with the wild-type strain *E. coli* 86-24INT.

None of the mice developed obvious diarrhea or visible blood in feces, although feces were discolored in sick mice. No symptoms were seen in the two mice inoculated with the control FN414 strain and in PBS controls.

The results suggest that the presence of Stx is essential for the development of neurological symptoms. The results also show that intimin contributed to symptoms and that an intact T3SS system is essential for the development of severe symptoms in this mouse model.

The effect of bacterial genotype on colonization and bacterial burden

Fecal cultures were taken from mice on days 1 and 4 after inoculation in order to address the importance of bacterial colonization and/or colonic persistence for the development of symptoms. The results for cultures taken on day 1 are summarized in Table 2 and show that most mice exhibited positive fecal cultures on day 1 regardless of the inoculated strain. Strain 86-24INT had the highest bacterial counts, followed by strain 87-23INT whereas strains UMD619FE and CVD451 had very low bacterial counts. Most mice did not have positive fecal cultures by day 4 even if symptomatic (data not shown).

Pathology in the colons of the sick mice

Proximal and distal colons were collected from 25 symptomatic mice inoculated with strains 86-24INT (n=6), 87-23INT (n=7), UMD619FE (n=4), UMD619$_{pCVD444}$INT (n=3), CVD451 (n=2), CVD451$_{pCVD446}$INT (n=3) and 14 asymptomatic mice 86-24INT (n=1), 87-23INT (n=1), UMD619FE (n=3), CVD451 (n=4), FN414 (n=1) and PBS controls (n=4). Colons from all symptomatic mice exhibited macroscopic hyperemia and sparsity of feces in comparison to colons from asymptomatic and control mice.

In symptomatic mice histopathological lesions exhibited predominantly inflammatory infiltrates in the distal colons of mice inoculated with strains 86-24INT (4 out of 6, indicating that 4 of 6 mice exhibited inflammatory infiltrates), 87-23INT (1 out of 7), UMD619FE (2 out of 4), UMD619$_{pCVD444}$INT (1 out of 3), CVD451 (1 out of 2), CVD451$_{pCVD446}$INT (3 out of 3) (see Figure S2a-c (SD). A comparison between the numbers of inflammatory infiltrates in the different groups is shown in Figure S3 (SD). Significantly more infiltrates were found in the distal colons of mice inoculated with strain 86-24INT compared to strain 87-23INT and PBS controls ($p< 0.05$ for both). In addition, vascular congestion was noted in the distal colons of all sick mice inoculated with strain 86-24INT (inset Figure S2a, SD) and with strain UMD619FE (data not shown). Distal colons were slightly hyperemic in mice inoculated with strains 87-23INT, CVD451, UMD619$_{pCVD444}$INT and CVD451$_{pCVD446}$INT. Goblet cells depletion was noted in symptomatic and asymptomatic mice with no correlation to the bacterial strain (data not shown).

Histopathologic examination of the proximal colons of all symptomatic mice revealed few inflammatory infiltrates in mice inoculated with 87-23INT (1 out of 7) and CVD451 (1 out of

2 data not shown). Furthermore, the interstitial space appeared shrunken indicating dehydration in most of sick mice (Figure S2d, SD). Asymptomatic mice as well as mice inoculated with strain FN414 and PBS-control mice exhibited normal histology (Figures S2e, f, SD).

Correlation of the inoculated strain with intestinal cell death

TUNEL assay was performed in proximal and distal colons obtained from mice inoculated with strains 86-24INT (n=5 with symptom score 3, n=1 with symptom score 2), 87-23INT (n=2 with symptom score 3, n=3 with symptom score 2, n=1 with symptom score 0), UMD619FE (n=1 with symptom score 3, n=2 with symptom score 2, n=3 with symptom score 0), CVD451 (n=2 with symptom score 2, n=4 with symptom score 0) and from control mice (FN414, n=1 and PBS controls, n=4). To obtain optimal comparison, sections from the same part of the intestine (proximal or distal) were taken from one mouse from each of the five groups and placed on the same slide. The results of TUNEL labelling are presented in Figure 3 demonstrating TUNEL positive cells in the mucosal epithelium of the proximal colon (Figures 3a and 3b, showing tissue from mice inoculated with 86-24INT and 87-23INT, respectively) and distal colon (Figure 3c, 86-24INT) as well as in mucosa-associated lymphatic tissue (Figure 3d, 86-24INT). In the PBS controls few TUNEL positive cells were visualized in the proximal colon (Figure 3e) and distal colon (not shown) as well as in the lymphatics (Figure 3f).

Caspase-3 assay was performed in sections obtained from sick mice inoculated with strains 86-24INT (distal colons n=5, proximal colons n=3), 87-23INT, UMD619FE, CVD451 and PBS controls (distal and proximal colons n=1 in each group). Few caspase-3 labelled cells

were found which were predominantly located in the epithelium or in the lumen in extruded cells (Figure 3g). Certain caspase-3 positive cells were also TUNEL positive (Figure 3h).

A comparison of the numbers of dying cells detected by the TUNEL assay in the colons of mice inoculated with the various bacteria strains is shown in Figure 4. All mice inoculated with *E. coli* O157:H7 strains (irrespective of symptom score) exhibited more dying cells compared to PBS control mice. The most pronounced cell death was found in proximal and distal colons of mice inoculated with the wild-type Stx2-producing 86-24INT strain compared to 87-23INT ($p < 0.01$ for both proximal and distal colon) or *escN* mutant ($p = 0.01$ proximal colon, $p < 0.01$ distal colon) and *eae* mutant ($p < 0.05$ for proximal colon and $p < 0.01$ for distal colon).

Discussion

Enterohemorrhagic *Escherichia coli* (EHEC) infection may lead to severe hemorrhagic colitis with gastro-intestinal complications. The two pediatric patients with HUS described here had a prolonged course of disease and developed colonic perforation. These patients exemplify the most severe course of intestinal affection during EHEC infection. We were able to demonstrate abundant cell death in their sigmoid colon using the TUNEL technique. From this we concluded that the cell death observed was, at least in part, due to apoptosis. Massive injury to the intestinal mucosa would allow bacterial virulence factors to gain access to the circulation. In an attempt to define which EHEC virulence factors contribute to intestinal cell death we used wild-type (Stx2-producing and non-producing) and mutated *E. coli* O157:H7 strains in a previously described mouse model [6]. The most pronounced cell death occurred in mice inoculated with the wild-type Stx2-producing 86-24INT strain. Less pronounced cell death was detected in mice inoculated with strain 87-23INT (the parent strain 87-23 was shown here to be isogenic to 86-24 apart from lacking Stx2) and in mice inoculated with strains UMD619FE and CVD451. The latter two strains exhibited reduced bacterial counts which could affect the toxin load released into the intestine. We thus conclude that intestinal cell injury was induced by Stx.

During interactions of EHEC with the intestinal commensal microflora Stx production can be induced by quorum sensing signaling [26], but also suppressed by the normal human microflora [27]. In vitro studies have shown that Stx causes apoptosis of human and murine intestinal epithelial cells in the distal colon [21, 28]. Furthermore, studies have shown that Stx may induce apoptosis in a variety of epithelial cells in vitro [29]. In addition to its effect on the intestine, Stx has been shown to have a cytotoxic effect and induce apoptosis of glomerular endothelial and epithelial cells [30, 31]. The current study indicates that these

findings also apply in vivo as we found distinct differences in the degree of intestinal cell death induced by the Stx-producing 86-24INT strain compared to the Stx-negative strain 87-23INT confirming the potential of Stx to induce colonic cell death in vivo during EHEC infection.

The effect of Stx is enhanced by TNF-α, IL-1, LPS and butyrate [31, 32]. Stx also exerts an apoptotic effect on human brain microvascular endothelial cells, even here the effect was increased by TNF-α which sensitized cells to Stx1 [33]. TNF-α upregulates the Gb3 receptor [32]. The presence of the Stx receptor determines the vulnerability of tissue to toxin-induced damage. The Gb3 receptor has been detected in the intestine of rabbits [34] and mice [35]. In mice the receptor was demonstrated in the epithelium of the distal colon [35] although mRNA was also detected in the small intestine [36]. Gb3-null mutant mice were protected from Stx's effects indicating the importance of Gb3 expression for targeting of Stx-induced cellular damage [37]. In this study marked cell death was noted in both the proximal and distal colons of mice inoculated with the Stx2-producing strain (86-24). As the proximal colon in the mouse does not bind Stx1 [35] this would suggest that not only actual Stx binding but also secondary immune responses in the intestine could have contributed to the tissue damage.

Intimin has been implicated in the development of diarrhea in a porcine model [38]. It is necessary for colonization of the human colon by most strains of *E. coli* O157, as demonstrated using in vitro organ cultures [39]. Using the mouse ileal loop model *E. coli* O157:H7 was found to induce attaching and effacing lesions in mouse intestine [40]. The presence of intimin and its receptor Tir were essential for this interaction to occur. A previous study showed that strain UMD619 was incapable of attaching intimately to colonic epithelial cells in newborn piglets and that the complemented strain $UMD619_{pCVD444}$ regained the

phenotype [38]. The results of the present investigation indicate that the same is true for this mouse model, that lack of intimin reduces bacterial counts. The Δ*eae* mutant developed less symptoms, as shown in Figure 2, and the strain complemented with intimin developed symptoms similar to the wild-type 86-24INT strain, presumably due to its increased ability to colonize.

The current study showed that the *eae* and *escN* mutants exhibited markedly reduced bacterial counts, intestinal cytotoxicity and virulence. The contributions of *eae* and *escN* to intestinal cell apoptosis have not been studied previously, although EspF, encoded on the LEE4 operon and regulated by *escN* [13] has been shown to induce host cell death via apoptosis [41]. We presume, however, that the decreased intestinal cell death observed in mice inoculated with strain CVD451 (with a mutation affecting *escN*) is primarily related to reduced bacterial counts, but cannot exclude the possible contribution of EspF to induction of cell death.

Using a *Citrobacter rodentium* model, Deng et al studied the importance of all 41 LEE genes for the virulence of the strain in mice [13]. They conclusively showed that the entire LEE was required for full virulence and that *C. rodentium* mutants Δ*eae* and Δ*escN* did not colonize adequately or exhibit virulence. Deletion of the entire LEE4 operon encoding type III secreted proteins impaired persistence of *E. coli* O157:H7 in cattle [42] and a deletion of *espA* markedly reduced the ability of *E. coli* O157:H7 to colonize the intestines of calves [43] and bind to cultured epithelial cells and induce actin rearrangements [44]. Likewise, an *escN* mutant of EPEC, which, as in EHEC is incapable of secreting Tir, Esps A, B and D, exhibited defective formation of attaching and effacing lesions in tissue culture cells. When complemented with the CVD446 plasmid carrying an intact *escN* gene from EPEC, the phenotype was restored [45]. The results presented herein are in agreement with these

previous studies and show that an intact T3SS was essential for the development of severe symptoms.

The mouse model used here was previously developed in our laboratory [6] and does not require streptomycin-treatment as has been described for other murine models of *E. coli* O157:H7 [8, 46]. Not all mice inoculated with *E. coli* O157:H7 developed symptoms. Other murine models have circumvented the issue of bacterial inoculation by treating mice with purified Stx [47]. We believe that the model described herein is more adequate for the study of *E. coli* O157:H7-induced intestinal infection as it would allow for quorum sensing signalling and cross-talk with the intestinal microflora to occur [26] because the mice were not pre-treated with an antibiotic. The separate contributions of the different virulence factors could be studied by genetic alterations of the parent strain. Interestingly, the Stx-negative strain 87-23INT also exhibited virulence. This observation has been made before [6] and suggests that *E. coli* O157:H7 possess multiple virulence factors. We could, however, show that Stx2 is important for the induction of intestinal cell death. Thus the mechanism by which strain 87-23INT induces severe symptoms in mice is presumably not entirely related to a cytotoxic effect on the intestinal epithelium.

A difference in the localization of cell death was noted when comparing human and murine intestines. In the human sigmoid colon TUNEL-positive cells were predominantly found in the lamina propria and in the vasculature while in the mouse colon they were mostly located in the mucosa-associated lymphatic tissue and epithelial cells. These differences could be related to Stx-receptor localization, as the human intestinal microvascular endothelial cells express high levels of the receptor [48]. In addition, differences could be due to the severe and prolonged hemorrhagic colitis seen in patients, whereas mice did not develop hemorrhagic

colitis. The longer time span between the onset of the infection and the removal of the colonic tissues in patients (16-27 days) in comparison to mice (2-4 days) could result in an increased cytokine response which would be expected to contribute to the extensive damage observed in the human sigmoid colon.

Intimin-specific antibodies can be detected in sera from patients after EHEC infection [49]. Anti–intimin antibodies have been shown to protect piglets from colonization with *E. coli* O157:H7 [50]. Intimin has been studied as a potential vaccine for protection against *E. coli* O157:H7 infection. Intimin-based vaccines confer protection in immunized mice [51]. In the present study we show that patients with EHEC infection exhibited massive intestinal cell death and that the specific *E. coli* O157:H7 virulence factors addressed were all likely to contribute to this process by promoting bacterial persistence and toxin-induced intestinal cell injury. Thus this study further suggests that *E. coli* O157:H7 adhesins and secreted proteins should be targeted as potential vaccines against bacterial colonization and intestinal injury.

Acknowledgements

The authors wish to thank Professor James Kaper of the Center for Vaccine Development, University of Maryland, Baltimore MD, for mutant strains and Professor Phil Tarr, Washington University, St Louis MO, for good advice. The technical assistance of Dr. Sofie Nordström was highly appreciated.

This study was presented as an oral presentation at ”Current diagnosis and therapy of Hemolytic Uremic Syndrome” Innsbruck, Austria, May 18-20, 2009 and as a poster at the 4 th International Workshop on Thrombotic Microangiopathies, Weimar, Germany, October 1-3, 2009.

References

1. Brandt JR, Fouser LS, Watkins SL, Zelikovic I, Tarr PI, Nazar-Stewart V, Avner ED (1994) Escherichia coli O 157:H7-associated hemolytic-uremic syndrome after ingestion of contaminated hamburgers. J Pediatr 125:519-526.
2. Richardson SE, Karmali MA, Becker LE, Smith CR (1988) The histopathology of the hemolytic uremic syndrome associated with verocytotoxin-producing Escherichia coli infections. Hum Pathol 19:1102-1108.
3. Dean-Nystrom EA, Bosworth BT, Cray WC, Jr., Moon HW (1997) Pathogenicity of Escherichia coli O157:H7 in the intestines of neonatal calves. Infect Immun 65:1842-1848.
4. Tzipori S, Wachsmuth IK, Chapman C, Birden R, Brittingham J, Jackson C, Hogg J (1986) The pathogenesis of hemorrhagic colitis caused by Escherichia coli O157:H7 in gnotobiotic piglets. J Infect Dis 154:712-716.
5. Pai CH, Kelly JK, Meyers GL (1986) Experimental infection of infant rabbits with verotoxin-producing Escherichia coli. Infect Immun 51:16-23.
6. Karpman D, Connell H, Svensson M, Scheutz F, Alm P, Svanborg C (1997) The role of lipopolysaccharide and Shiga-like toxin in a mouse model of Escherichia coli O157:H7 infection. J Infect Dis 175:611-620.
7. Taguchi H, Takahashi M, Yamaguchi H, Osaki T, Komatsu A, Fujioka Y, Kamiya S (2002) Experimental infection of germ-free mice with hyper-toxigenic enterohaemorrhagic Escherichia coli O157:H7, strain 6. J Med Microbiol 51:336-343.
8. Calderon Toledo C, Rogers TJ, Svensson M, Tati R, Fischer H, Svanborg C, Karpman D (2008) Shiga toxin-mediated disease in MyD88-deficient mice infected with Escherichia coli O157:H7. Am J Pathol 173:1428-1439.

9. Phillips AD, Navabpour S, Hicks S, Dougan G, Wallis T, Frankel G (2000) Enterohaemorrhagic Escherichia coli O157:H7 target Peyer's patches in humans and cause attaching/effacing lesions in both human and bovine intestine. Gut 47:377-381.

10. Chong Y, Fitzhenry R, Heuschkel R, Torrente F, Frankel G, Phillips AD (2007) Human intestinal tissue tropism in Escherichia coli O157 : H7--initial colonization of terminal ileum and Peyer's patches and minimal colonic adhesion ex vivo. Microbiology 153:794-802.

11. Nataro JP, Kaper JB (1998) Diarrheagenic Escherichia coli. Clin Microbiol Rev 11:142-201.

12. Jerse AE, Yu J, Tall BD, Kaper JB (1990) A genetic locus of enteropathogenic Escherichia coli necessary for the production of attaching and effacing lesions on tissue culture cells. Proc Natl Acad Sci USA 87:7839-7843.

13. Deng W, Puente JL, Gruenheid S, Li Y, Vallance BA, Vazquez A, Barba J, Ibarra JA, O'Donnell P, Metalnikov P, Ashman K, Lee S, Goode D, Pawson T, Finlay BB (2004) Dissecting virulence: systematic and functional analyses of a pathogenicity island. Proc Natl Acad Sci USA 101:3597-3602.

14. Garmendia J, Phillips AD, Carlier MF, Chong Y, Schuller S, Marches O, Dahan S, Oswald E, Shaw RK, Knutton S, Frankel G (2004) TccP is an enterohaemorrhagic Escherichia coli O157:H7 type III effector protein that couples Tir to the actin-cytoskeleton. Cell Microbiol 6:1167-1183.

15. Frankel G, Phillips AD, Rosenshine I, Dougan G, Kaper JB, Knutton S (1998) Enteropathogenic and enterohaemorrhagic Escherichia coli: more subversive elements. Mol Microbiol 30:911-921.

16. O'Brien AD, Holmes RK (1987) Shiga and Shiga-like toxins. Microbiol Rev 51:206-220.

17. Schuller S, Heuschkel R, Torrente F, Kaper JB, Phillips AD (2007) Shiga toxin binding in normal and inflamed human intestinal mucosa. Microbes Infect 9:35-39.

18. Thorpe CM, Hurley BP, Lincicome LL, Jacewicz MS, Keusch GT, Acheson DW (1999) Shiga toxins stimulate secretion of interleukin-8 from intestinal epithelial cells. Infect Immun 67:5985-5993.

19. Hurley BP, Jacewicz M, Thorpe CM, Lincicome LL, King AJ, Keusch GT, Acheson DW (1999) Shiga toxins 1 and 2 translocate differently across polarized intestinal epithelial cells. Infect Immun 67:6670-6677.

20. Keenan KP, Sharpnack DD, Collins H, Formal SB, O'Brien AD (1986) Morphologic evaluation of the effects of Shiga toxin and E coli Shiga-like toxin on the rabbit intestine. Am J Pathol 125:69-80.

21. Schuller S, Frankel G, Phillips AD (2004) Interaction of Shiga toxin from Escherichia coli with human intestinal epithelial cell lines and explants: Stx2 induces epithelial damage in organ culture. Cell Microbiol 6:289-301.

22. Schmitt R, Carlsson F, Morgelin M, Tati R, Lindahl G, Karpman D Tissue deposits of IgA-binding streptococcal M proteins in IgA nephropathy and Henoch-Schonlein purpura. Am J Pathol 176:608-618.

23. O'Brien AD, Melton AR, Schmitt CK, McKee ML, Batts ML, Griffin DE (1993) Profile of Escherichia coli O157:H7 pathogen responsible for hamburger-borne outbreak of hemorrhagic colitis and hemolytic uremic syndrome in Washington. J Clin Microbiol 31:2799-2801.

24. Perez MT, Arner K, Håkansson A (1997) DNA fragmentation characteristic of apoptosis and cell loss induced by kainic acid in rabbit retinas. Neurochem Int 31:251-260.

25. Karpman D, Håkansson A, Perez MT, Isaksson C, Carlemalm E, Caprioli A, Svanborg C (1998) Apoptosis of renal cortical cells in the hemolytic-uremic syndrome: in vivo and in vitro studies. Infect Immun 66:636-644.

26. Hughes DT, Clarke MB, Yamamoto K, Rasko DA, Sperandio V (2009) The QseC adrenergic signaling cascade in Enterohemorrhagic E. coli (EHEC). PLoS Pathog 5:e1000553.

27. Bellmeyer A, Cotton C, Kanteti R, Koutsouris A, Viswanathan VK, Hecht G (2009) Enterohemorrhagic Escherichia coli suppresses inflammatory response to cytokines and its own toxin. Am J Physiol Gastrointest Liver Physiol 297:G576-581.

28. Kashiwamura M, Kurohane K, Tanikawa T, Deguchi A, Miyamoto D, Imai Y (2009) Shiga toxin kills epithelial cells isolated from distal but not proximal part of mouse colon. Biol Pharm Bull 32:1614-1617.

29. Cherla RP, Lee SY, Tesh VL (2003) Shiga toxins and apoptosis. FEMS Microbiol Lett 228:159-166.

30. Pijpers AH, van Setten PA, van den Heuvel LP, Assmann KJ, Dijkman HB, Pennings AH, Monnens LA, van Hinsbergh VW (2001) Verocytotoxin-induced apoptosis of human microvascular endothelial cells. J Am Soc Nephrol 12:767-778.

31. Hughes AK, Stricklett PK, Schmid D, Kohan DE (2000) Cytotoxic effect of Shiga toxin-1 on human glomerular epithelial cells. Kidney Int 57:2350-2359.

32. van de Kar NC, Monnens LA, Karmali MA, van Hinsbergh VW (1992) Tumor necrosis factor and interleukin-1 induce expression of the verocytotoxin receptor globotriaosylceramide on human endothelial cells: implications for the pathogenesis of the hemolytic uremic syndrome. Blood 80:2755-2764.

33. Ergonul Z, Hughes AK, Kohan DE (2003) Induction of apoptosis of human brain microvascular endothelial cells by shiga toxin 1. J Infect Dis 187:154-158.

34. Zoja C, Corna D, Farina C, Sacchi G, Lingwood C, Doyle MP, Padhye VV, Abbate M, Remuzzi G (1992) Verotoxin glycolipid receptors determine the localization of microangiopathic process in rabbits given verotoxin-1. J Lab Clin Med 120:229-238.

35. Imai Y, Fukui T, Kurohane K, Miyamoto D, Suzuki Y, Ishikawa T, Ono Y, Miyake M (2003) Restricted expression of shiga toxin binding sites on mucosal epithelium of mouse distal colon. Infect Immun 71:985-990.

36. Fujii Y, Numata S, Nakamura Y, Honda T, Furukawa K, Urano T, Wiels J, Uchikawa M, Ozaki N, Matsuo S, Sugiura Y (2005) Murine glycosyltransferases responsible for the expression of globo-series glycolipids: cDNA structures, mRNA expression, and distribution of their products. Glycobiology 15:1257-1267.

37. Okuda T, Tokuda N, Numata S, Ito M, Ohta M, Kawamura K, Wiels J, Urano T, Tajima O, Furukawa K (2006) Targeted disruption of Gb3/CD77 synthase gene resulted in the complete deletion of globo-series glycosphingolipids and loss of sensitivity to verotoxins. J Biol Chem 281:10230-10235.

38. Tzipori S, Gunzer F, Donnenberg MS, de Montigny L, Kaper JB, Donohue-Rolfe A (1995) The role of the eaeA gene in diarrhea and neurological complications in a gnotobiotic piglet model of enterohemorrhagic Escherichia coli infection. Infect Immun 63:3621-3627.

39. Mundy R, Schuller S, Girard F, Fairbrother JM, Phillips AD, Frankel G (2007) Functional studies of intimin in vivo and ex vivo: implications for host specificity and tissue tropism. Microbiology 153:959-967.

40. Girard F, Frankel G, Phillips AD, Cooley W, Weyer U, Dugdale AH, Woodward MJ, La Ragione RM (2008) Interaction of enterohemorrhagic Escherichia coli O157:H7 with mouse intestinal mucosa. FEMS Microbiol Lett 283:196-202.

41. Crane JK, McNamara BP, Donnenberg MS (2001) Role of EspF in host cell death induced by enteropathogenic Escherichia coli. Cell Microbiol 3:197-211.

42. Naylor SW, Roe AJ, Nart P, Spears K, Smith DG, Low JC, Gally DL (2005) Escherichia coli O157 : H7 forms attaching and effacing lesions at the terminal rectum of cattle and colonization requires the LEE4 operon. Microbiology 151:2773-2781.

43. Dziva F, Vlisidou I, Crepin VF, Wallis TS, Frankel G, Stevens MP (2007) Vaccination of calves with EspA, a key colonisation factor of Escherichia coli O157:H7, induces antigen-specific humoral responses but does not confer protection against intestinal colonisation. Vet Microbiol 123:254-261.

44. Ebel F, Podzadel T, Rohde M, Kresse AU, Kramer S, Deibel C, Guzman CA, Chakraborty T (1998) Initial binding of Shiga toxin-producing Escherichia coli to host cells and subsequent induction of actin rearrangements depend on filamentous EspA-containing surface appendages. Mol Microbiol 30:147-161.

45. Jarvis KG, Giron JA, Jerse AE, McDaniel TK, Donnenberg MS, Kaper JB (1995) Enteropathogenic Escherichia coli contains a putative type III secretion system necessary for the export of proteins involved in attaching and effacing lesion formation. Proc Natl Acad Sci USA 92:7996-8000.

46. Wadolkowski EA, Burris JA, O'Brien AD (1990) Mouse model for colonization and disease caused by enterohemorrhagic Escherichia coli O157:H7. Infect Immun 58:2438-2445.

47. Keepers TR, Psotka MA, Gross LK, Obrig TG (2006) A murine model of HUS: Shiga toxin with lipopolysaccharide mimics the renal damage and physiologic response of human disease. J Am Soc Nephrol 17:3404-3414.

48. Jacewicz MS, Acheson DW, Binion DG, West GA, Lincicome LL, Fiocchi C, Keusch GT (1999) Responses of human intestinal microvascular endothelial cells to Shiga toxins 1 and 2 and pathogenesis of hemorrhagic colitis. Infect Immun 67:1439-1444.

49. Jenkins C, Chart H, Smith HR, Hartland EL, Batchelor M, Delahay RM, Dougan G, Frankel G (2000) Antibody response of patients infected with verocytotoxin-producing Escherichia coli to protein antigens encoded on the LEE locus. J Med Microbiol 49:97-101.

50. Dean-Nystrom EA, Gansheroff LJ, Mills M, Moon HW, O'Brien AD (2002) Vaccination of pregnant dams with intimin(O157) protects suckling piglets from Escherichia coli O157:H7 infection. Infect Immun 70:2414-2418.

51. Judge NA, Mason HS, O'Brien AD (2004) Plant cell-based intimin vaccine given orally to mice primed with intimin reduces time of Escherichia coli O157:H7 shedding in feces. Infect Immun 72:168-175.

52. Svenungsson B, Lagergren A, Ekwall E, Evengard B, Hedlund KO, Karnell A, Lofdahl S, Svensson L, Weintraub A (2000) Enteropathogens in adult patients with diarrhea and healthy control subjects: a 1-year prospective study in a Swedish clinic for infectious diseases. Clin Infect Dis 30:770-778.

53. Caprioli A, Luzzi I, Rosmini F, Pasquini P, Cirrincione R, Gianviti A, Matteucci MC, Rizzoni G (1992) Hemolytic-uremic syndrome and Vero cytotoxin-producing Escherichia coli infection in Italy. The HUS Italian Study Group. J Infect Dis 166:154-158.

54. Sjögren AC, Kaper JB, Caprioli A, Karpman D (2004) Enzyme-linked immunosorbent assay for detection of Shiga toxin-producing Escherichia coli infection by antibodies to Escherichia coli secreted protein B in children with hemolytic uremic syndrome. Eur J Clin Microbiol Infect Dis 23:208-211.

Table 1: Subjects investigated in this study

Subject	Sex	Age years	Clinical symptoms	Laboratory findings	EHEC diagnostics	Colon tissue obtained
Patient 1	M	9	Bloody diarrhea Renal failure Pneumonia Peritonitis[a]	Hemoglobin 66 g/L[b] Platelets 27 x 10^9/L[b] Creatinine 461 µmol/L[b] LDH 98 µkat/L[b]	Fecal *E. coli* O157:H7 strain *stx2, eae* positive[c] on day 14 after onset of diarrhea. Bacteria had cleared from stool by day of surgery	Partial sigmoidectomy on day 27 after onset of diarrhea, day 25 after onset of HUS
Patient 2	F	10	Bloody diarrhea Renal failure Seizures Peritonitis[a]	Hemoglobin 51 g/L[b] Platelets 39 x 10^9/L[b] Creatinine 394 µmol/L[b] LDH 83 µkat/L[b]	Fecal isolate not obtained Serum antibodies to O157LPS negative[d]. Serum IgA antibodies to EspB positive[e]	Partial sigmoidectomy on day 16 after onset of diarrhea, day 13 after onset of HUS
Control 1	F	1	Sigmoidostomy because of anal atresia	NA	NA	Area adjacent to the sigmoidostomy
Control 2	F	14	Celiac disease in remission	NA	NA	Biopsy taken to rule out IBD[f]
Control 3	M	7	Hemorrhoids	NA	NA	Biopsy taken due to gastrointestinal bleeding[f]

M, male, F, female, NA, not applicable. IBD, inflammatory bowel disease. a, both patients received antibiotics consisting of intraperitoneal Vancomycin and Tobramycin as well as intravenous Meropenem at the time of colonic resection , b, reference values: hemoglobin 105 – 150 g/L, platelet count 140 – 400 x 10^9/L, creatinine 22 - 68 µmol/L, LDH (lactic dehydrogenase) < 12 µkat/L. c, assayed as per Svenungsson et al. [52]. d, assayed as per Caprioli et al. [53]. e, This patient had one episode of HUS following bloody diarrhea and has not had a recurrence in over 10 years. An EHEC strain was not isolated from the stool and serology was negative for antibodies to O157LPS. The patient was assumed to have an EHEC infection based on the clinical course and on serologic finding of IgA antibodies to EspB assayed as per Sjögren et al. [54]. f, The precise region of the resected colonic tissue is, at present, unknown.

Table 2. Numbers of sick mice, fecal cultures and bacterial counts in mice inoculated with each respective strain

EHEC strain	Total number of inoculated mice	Number of sick mice during the entire experiment (percent of total)	Sick day 1	Positive fecal culture day 1		Bacterial counts CFU/mg feces on day 1	
				Symptomatic	Asymptomatic	Median	Range
86-24INT (Stx2+)	25	20 (80 %)	20	19	4	12987	1860-130337[a]
87-23INT (Stx-)	20	15 (75 %)	15	13	4	1388	134 – 3827[b]
UMD619FE (*eae* mutant)	25	10 (40 %)	7	7	10	5	0 – 395 [c]
UMD619$_{pCVD444}$INT	10	6 (60 %)	4	4	4	NA	NA
CVD451 (*escN* mutant)	23	7 (30 %)	7	6/6[d]	8/9[d]	0	0 – 744[e]
CVD451$_{pCVD446}$INT	10	5 (50 %)	2	2	7	NA	NA

[a], 5 mice.[b], 3 mice.[c], 5 mice.[d], not all mice in this group were cultured, the denominator is equivalent to the number of cultured mice in this group on day 1. [e], 5 mice. NA: not assayed

Figure Legends

Figure 1. Intestinal pathology in patients with EHEC-associated HUS. Sigmoid colon was partly removed from two patients with EHEC infection. Panels **a**, **f,** and **h** show light microscopy from Patient 1 (as per Table 1) and panel **b** shows sigmoid colon from Patient 2 (all stained with hematoxylin-eosin). Patient tissues exhibited hemorrhages (short arrows), edema (long arrow), inflammatory infiltrates (the area in the red box at the lower left of panel a is enlarged in the inset) and necrosis in the colonic submucosa (visible in panel **b**). Panel **d** shows light microscopy from Control 1 stained with hematoxylin-eosin. Panels **c**, **e** and **g** show terminal deoxynucleotidyl transferase (TdT)-mediated dUPT-biotin nick-end-labelling (TUNEL) labeling in tissue from Patient 1 (panels **e** and **g**) and Control 1 (**c)**. Abundant TUNEL-labelling was detected in the lamina propria (**e**, see arrow) and in blood vessels (**g**, see arrow). Few TUNEL positive cells were noted in the normal colonic mucosa (**c,** see arrow). Magnification x 50 (**a**), x 200 (**b**-**f**), x 400 (**g**, **h**).

Figure 2. Symptoms in inoculated mice. A symptom score of 0 – 4 (as per Table S4, see SD) was assigned each mouse during the 5-day observation period. The highest score is shown for each individual mouse as well as medians for the group. Severe symptoms developed in mice inoculated with strains 86-24INT and 87-23INT. Few mice inoculated with the mutant strains developed severe symptoms. *, $P < 0.01$. Mice inoculated with each *E. coli* O157:H7 strain were also statistically compared with PBS controls, for 86-24INT, 87-23INT and UMD619$_{pCVD444}$INT $P < 0.01$ and CVD451$_{pCVD446}$INT $P = 0.01$, for UMD619FE $P < 0.05$, comparison with CVD451 was non-significant ($P = 0.07$).

Figure 3. TUNEL and caspase-3 labelling in colons of inoculated mice. TUNEL-labelling in the proximal (**a**) and distal colon (**c**) of mice inoculated with strain 86-24INT compared

with the proximal colon of a mouse inoculated with 87-23INT (**b**). The most abundant TUNEL-labelling was seen in the mucosa-associated lymphatic tissue of mice inoculated with strain 86-24INT (**d**). Few positive cells were seen in the proximal colon (e) as well as in the distal colon (not shown) and lymphatic tissue (f) of PBS-control mice. Caspase-3 labelling in the epithelium and in the extruded cells in the lumen (panel **g**, see arrows) in the distal colon of a mouse inoculated with strain 86-24INT and the same area with TUNEL-positive cells (panel **h**, see arrows). Magnification x 200 (**a,b,c,e**); x 400 (**d,f,g,h**).

Figure 4. Cell death in colons of inoculated mice. Cell death was assessed in sections obtained from mice inoculated with strains 86-24INT, 87-23INT, UMD619FE, CVD451 and from control mice (FN414 and PBS controls). The number of investigated mice is given under each bacterial strain. TUNEL positive cells were quantitated within an area of 1-11 mm^2. Values were expressed as the number of TUNEL-positive cells per 100 000 μm^2 of colonic tissue. The line inside each box represents the median. The upper and lower limits of the box-plot represent the interquartile range. The upper and lower limits represent the range. Outliers are marked with open circles. Significantly more TUNEL-positive cells were found in proximal and distal colons of mice inoculated with strain 86-24INT compared to the other strains and the PBS controls .*, $P < 0.05$; **, $P \leq 0.01$.

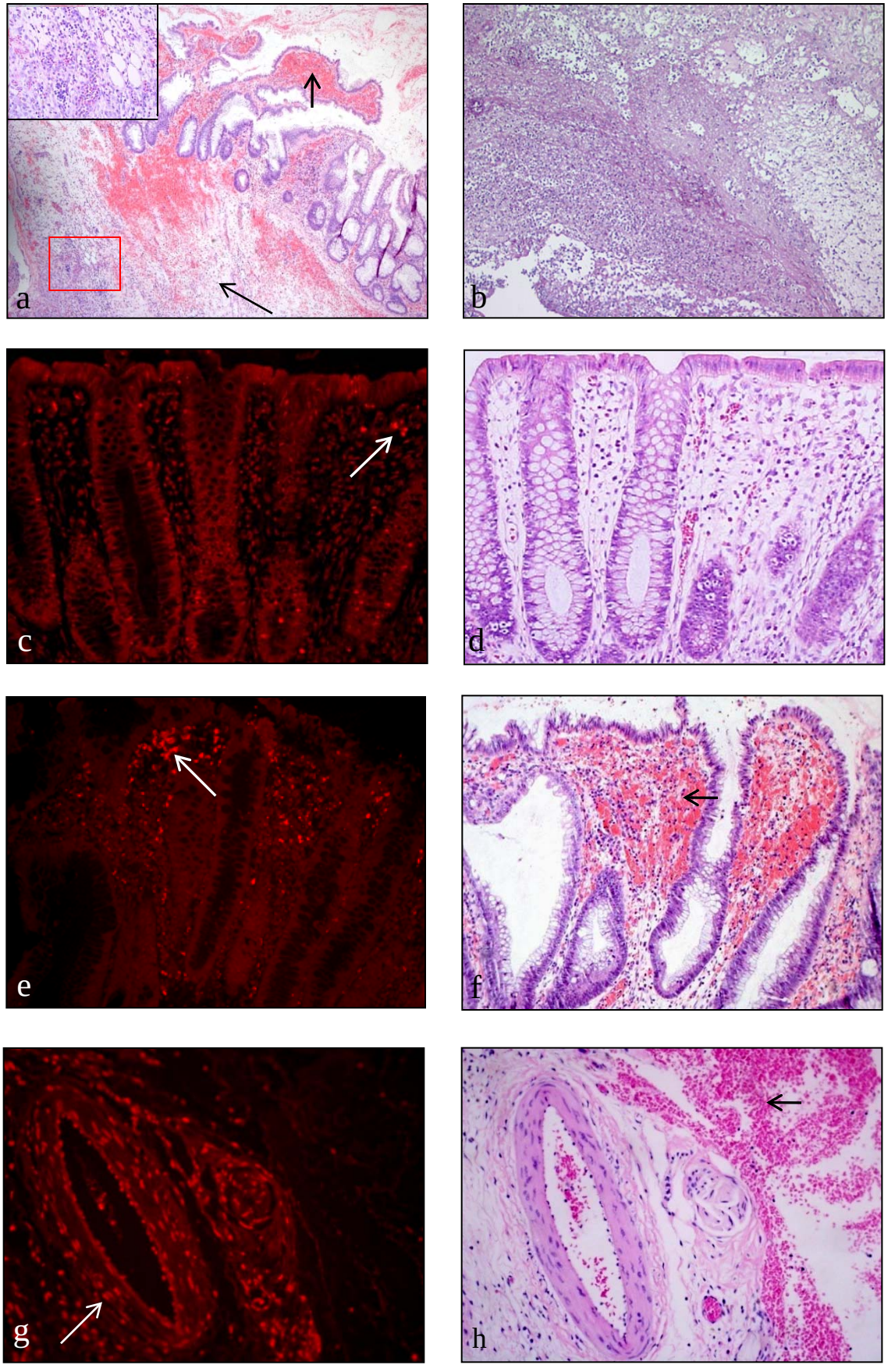

Figure 1

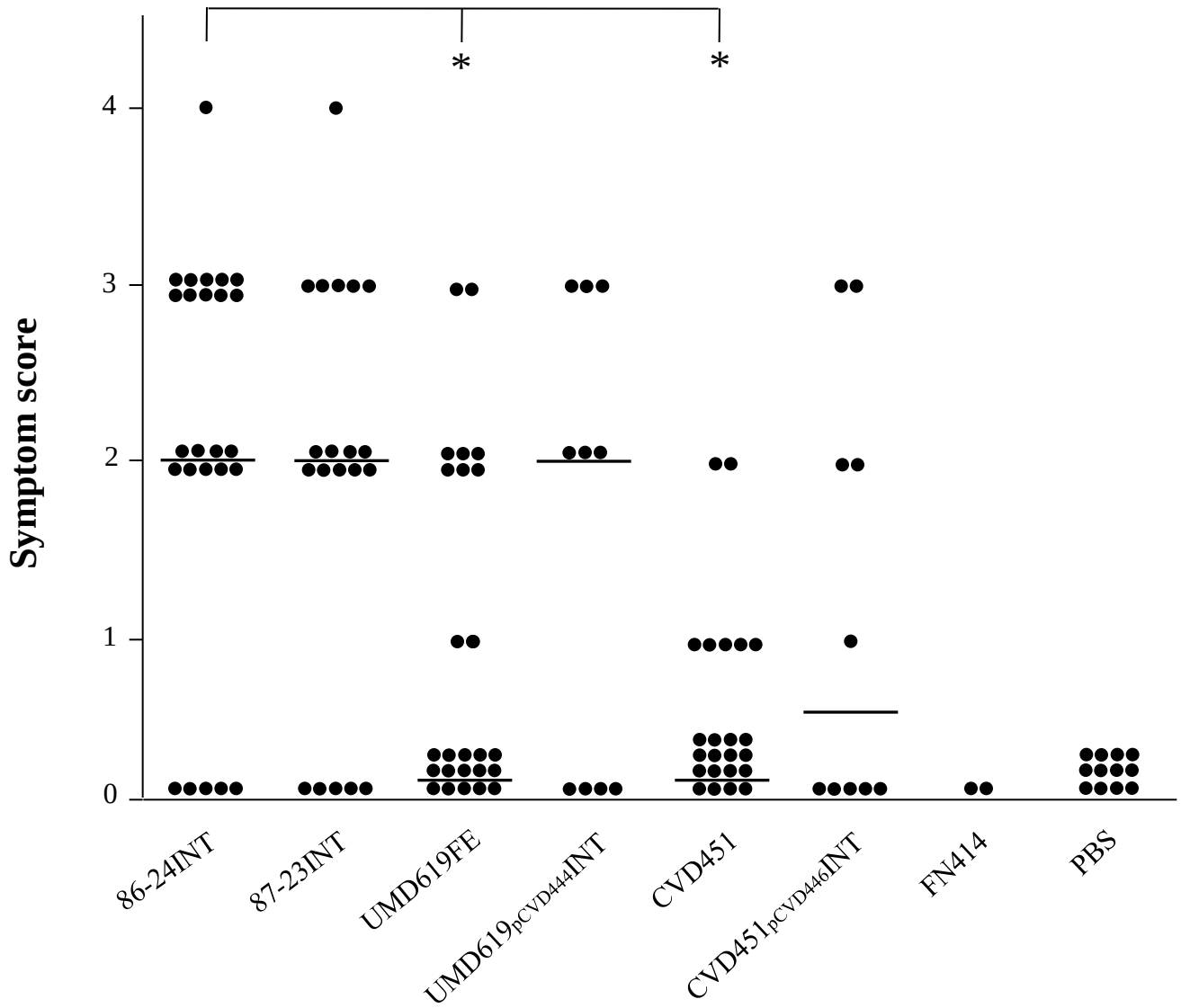
*
*
4
3
2
1
0
Symptom score
86-24INT
87-23INT
UMD619FE
UMD619pCVD444INT
CVD451
CVD451pCVD446INT
FN414
PBS
Inoculated strain

Figure 2

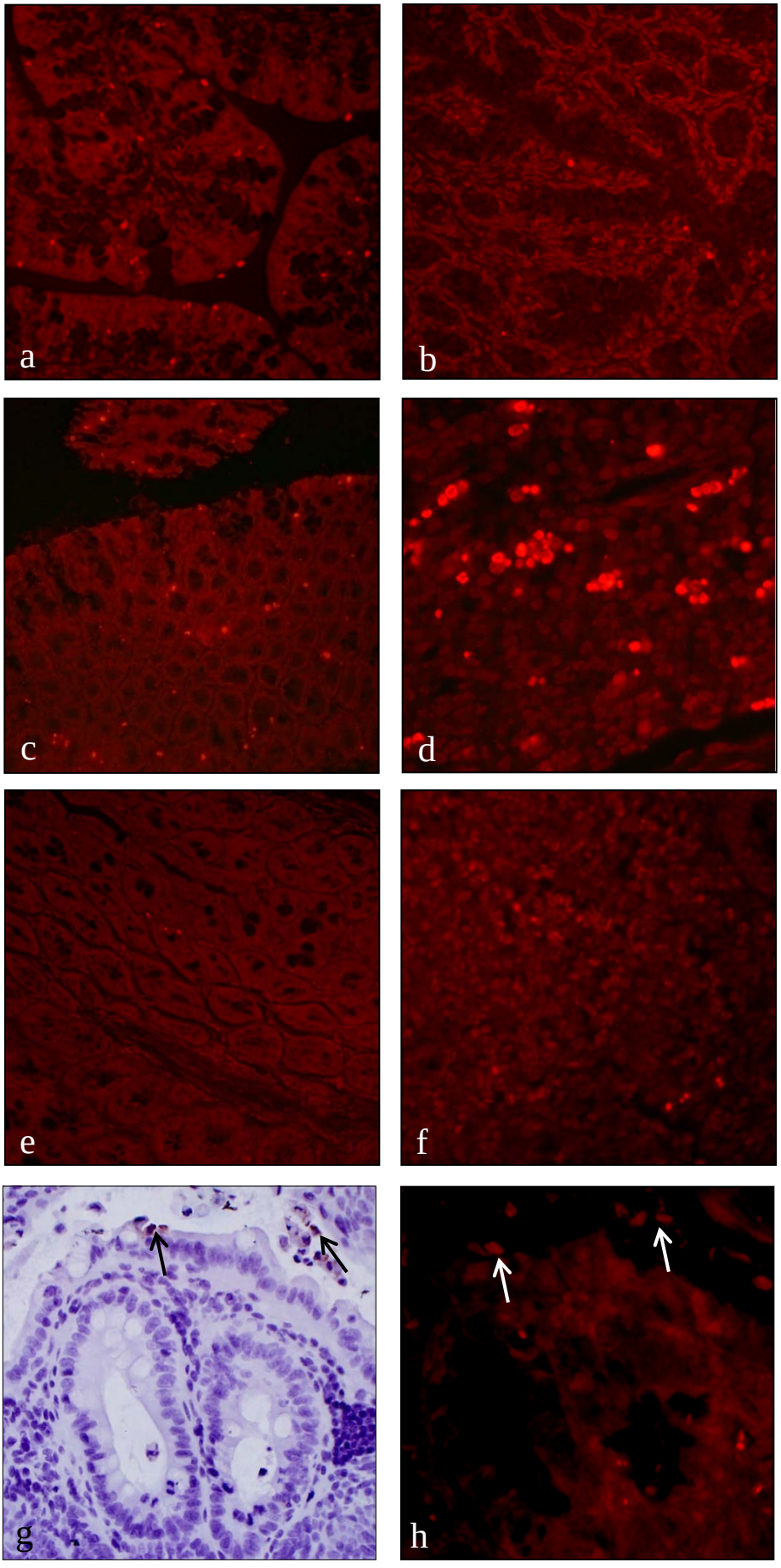

Figure 3

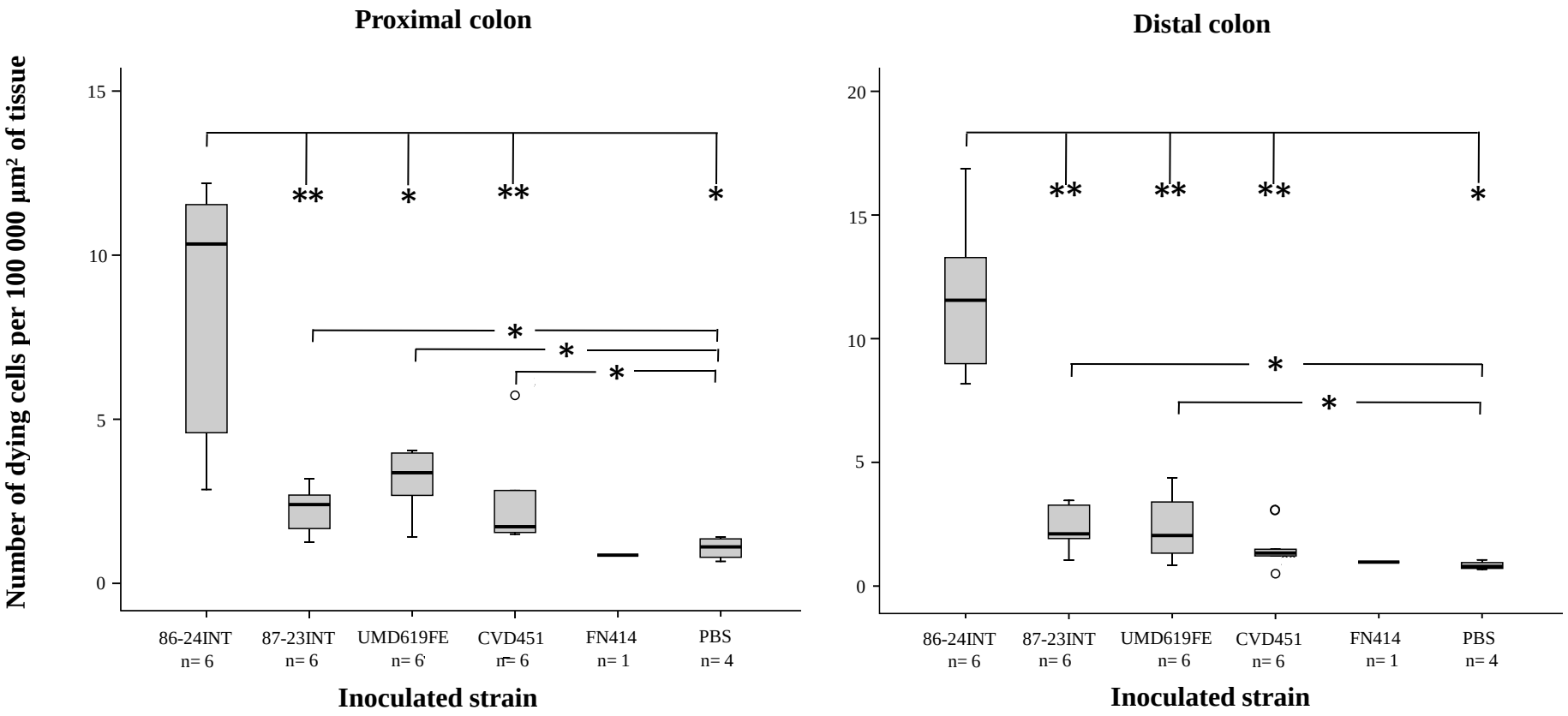
Proximal colon
Distal colon
Number of dying cells per 100 000 µm² of tissue
15
10
5
0
20
15
10
5
0
**
*
**
*
*
*
*
**
**
**
*
*
*
86-24INT
n= 6
87-23INT
n= 6
UMD619FE
n= 6
CVD451
n= 6
FN414
n= 1
PBS
n= 4
Inoculated strain

Figure 4

Supplementary methods

Detection of CD14 in human intestines

Sections were boiled for 15 minutes in 10 mM Tris/1mM EDTA buffer (KEBO Labs, VWR Stockholm, Sweden) pH 9.0 in a microwave oven to enhance antigenicity. The primary antibody was monoclonal mouse-anti human CD14 (Acris Antibodies, Herford, Germany) followed by secondary anti-mouse IgG conjugated to horseradish-peroxidise (Envision^{+}-system, DakoCytomation, Glostrup, Denmark).

Determination of the isogenicity of *E. coli* O157:H7 strains 86-24 and 87-23

To determine if the strains 86-24 and 87-23 were isogenic, three synonymous and three nonsynonymous single nucleotide polymorphism (SNP) locations were randomly chosen from the 31 backbone SNPs that arose on the phylogenetic branch leading to 86-24 as it radiated away from the founder of Cluster 2 [1]. Sites were amplified by PCR and sequenced. The two strains demonstrated isogenicity at each of these sites (Table S2).

Bacterial counts assayed by colony hybridization

Fecal samples were collected from mice inoculated with strains 86-24INT, 87-23INT, UMD619FE and CVD451, 24h after inoculation. Feces were weighed and homogenized in 1 ml sterile PBS. Serial dilutions were plated onto MacConkey agar plates and EHEC colony forming units were detected by colony hybridization. Colonies from plates were directly blotted onto nylon membranes (Hybond N+; GE Healthcare, Buckinghamshire, UK), treated with 0.5 M NaOH, washed twice with 5X Na_3 Citrate buffer (as per the manufacturer) and

allowed to dry until assayed. Filters were hybridized with a nucleic acid probe for specific detection of EHEC colonies based on the sequence of the *rfb* region. For probe construction, the *rfb* region was amplified by PCR using forward primer: 5'AAGATTGCGCTGAAGCCTTTG3' and reverse primer 5'CATTGGCATCGTGTGGAC-AG3' that amplify sequences within $rfbE_{EcO157:H7}$ [2]. Strains 86-24INT, 87-23INT, UMD619FE, CVD451 and FN414 (as a negative control) were first subject to analysis by PCR for the presence of the *rfb* region. Strain 86-24INT was selected for purification of the *rfb* probe using the QIAquick gel extraction kit (Qiagen, Hilden, Germany). Filters were processed and the *rfb* probe was labelled using the Amersham ECL direct nucleic acid labelling and detection kit (GE Healthcare, Buckinghamshire, UK). EHEC colony forming units were visualized and expressed per mg of feces.

TUNEL assay

Deparaffinized 3 µm sections were incubated for 30 min at 37°C with pepsin (3460U/mg; Sigma-Aldrich, Steinheim, Germany) in Tris-HCl buffer (pH 8.0). The sections were then incubated with TdT (50 U/µl) and biotinylated dUTP (16.4 µM biotin-16-dUTP, Roche, Mannheim Germany) in TdT buffer at 37°C for 60 min. The reaction was terminated by 2X SSC buffer (300 mM NaCl, 30 mM sodium citrate, ph 7,3) after which sections were rinsed, incubated with Streptavidin/Cy3 (1:9000, Jackson ImmunoResearch, Amersham, Baltimore, MD), and mounted with Vectashield containing DAPI (4', 6-diamidino-2-phenylindole) for labelling of nuclei (Vector Laboratories, Burlingame, CA). Control assays included pre-incubation of sections with DNase (2 µg/ml; Sigma-Aldrich) for 10 min, which resulted in strong positive labelling of all nuclei (positive control), and omission of biotin-labelled nucleotide which resulted in no detectable signal (negative control).

1. Leopold SR, Magrini V, Holt NJ, Shaikh N, Mardis ER, Cagno J, Ogura Y, Iguchi A, Hayashi T, Mellmann A, Karch H, Besser TE, Sawyer SA, Whittam TS, Tarr PI (2009) A precise reconstruction of the emergence and constrained radiations of Escherichia coli O157 portrayed by backbone concatenomic analysis. Proc Natl Acad Sci U S A 106:8713-8718.
2. Desmarchelier PM, Bilge SS, Fegan N, Mills L, Vary JC, Jr., Tarr PI (1998) A PCR specific for Escherichia coli O157 based on the rfb locus encoding O157 lipopolysaccharide. J Clin Microbiol 36:1801-1804.

Supplementary tables

Table S1: Bacterial strains used in this study

E. coli strain	Serotype	Characteristics	Stx	*eae*[a]	*escN*[b]	Antibiotic resistance	Reference
86-24	O157:H7	Wild-type	Stx2 +	+	+	-	[1, 2]
87-23	O157:H7	Wild-type	Stx -	+	+	-	[1, 2]
UMD619	O157:H7	86-24 with deletion mutation Δ*eae*	Stx2 +	-	+	Tc	[3]
UMD619$_{pCVD444}$	O157:H7	UMD619 complemented with plasmid CVD444 containing *eae* from EHEC strain EDL933	Stx2 +	+	+	Tc, Amp	[3]
CVD451	O157:H7	86-24 with insertion mutation affecting *escN*	Stx2 +	+	-	Str, Kn	[4]
CVD451$_{pCVD446}$	O157:H7	CVD451 complemented with plasmid CVD446 containing *escN* from EPEC strain E2348/69	Stx2 +	+	+	Str, Kn, Amp	[4, 5]
FN 414	OR:KN:H25	Control strain	Stx-	-	-	-	[1]

a, encodes the adhesin intimin [6, 7], b, encodes the regulation of the T3SS [7]. Tc, tetracycline; Amp, ampicillin; Str, streptomycin; Kn, kanamycin.

Table S2: Single nucleotide polymorphism typing of wild type strains

Amino acid change	Location[a]	86-24 [b]	87-23[b]	0157 Sakai [c]	Forward primer	Reverse primer
Synonymous	3798	T	T	G	AATGAGCAGGTCAGCTTTGC	GACATCGCTTTCAACATTGG
Synonymous	4259164	G	G	A	GGTTTTACCGTTGGTTTTGC	AATCAGCGTAGCCATTACCG
Synonymous	5391618	A	A	C	AAAATGGCTCCTTGTTGTGG	TGGTTGAAGCCTTTCGTAGG
Nonsynonymous	30477	T	T	C	ACGCTAAAACTCGACGATGG	ATGCTGATAGCGCGGTCTAC
Nonsynonymous	1330848	A	A	G	CCGCCAACAATCCACATAAT	CATCCCTCAGGCTAAAGACAA
Nonsynonymous	5103324	A	A	G	GAACCAGGCGTGATGAGTG	AACTTTCCGTGTCGTTGAGC

a, Location in reference to the fully sequenced Sakai strain. b, Radial c, Ancestral

Table S3: *E. coli* strain and number of mice used to obtain positive cultures from colon or feces

***E. coli* strain obtained after passage through mice**	**Total number of inoculated mice**	**Sick**	**Culture from intestine in sick mouse**	**Culture from feces in sick mouse**
86-24INT(*stx2+*)	2	1	1	1[a]
87-23INT *(stx-)*	2	1	1	1[a]
UMD619FE *(eae* mutant)	7	2	0	1
UMD619$_{\text{pCVD444}}$INT	3	1	1[a]	1[a]
CVD451 *(escN* mutant) parental strain	8	0	0	0
CVD451$_{\text{pCVD446}}$INT	4	2	1[a]	2[a]

a, these strains grew in both the colonic and fecal cultures. The colonic strain was termed “INT” and used in further experiments.

Table S4: Disease symptom score in inoculated mice (modified from [8])

Score	Characterization	Symptoms
0	No symptoms	-
1	Mild symptoms[a]	Systemic: Ruffled fur [b] Neurologic: none
2	Moderate symptoms	Systemic: Ruffled fur, hunched posture, decreased activity, squinting. Neurologic: none.
3	Severe symptoms	Systemic: Ruffled fur, hunched posture, severely decreased mobility, squinting, lethargy. Neurologic: ataxia, rigidity.
4	Death	

a, Mice that exhibited only mild symptoms, did not show further signs of illness and recovered.

b, Ruffled fur could occur transiently during the first 24 hours after inoculation and if temporary was not considered a symptom.

References

1. Karpman D, Connell H, Svensson M, Scheutz F, Alm P, Svanborg C (1997) The role of lipopolysaccharide and Shiga-like toxin in a mouse model of Escherichia coli O157:H7 infection. J Infect Dis 175:611-620.
2. Tarr PI, Neill MA, Clausen CR, Newland JW, Neill RJ, Moseley SL (1989) Genotypic variation in pathogenic Escherichia coli O157:H7 isolated from patients in Washington, 1984-1987. J Infect Dis 159:344-347.
3. Donnenberg MS, Tzipori S, McKee ML, O'Brien AD, Alroy J, Kaper JB (1993) The role of the eae gene of enterohemorrhagic Escherichia coli in intimate attachment in vitro and in a porcine model. J Clin Invest 92:1418-1424.
4. Jarvis KG, Kaper JB (1996) Secretion of extracellular proteins by enterohemorrhagic Escherichia coli via a putative type III secretion system. Infect Immun 64:4826-4829.
5. Jarvis KG, Giron JA, Jerse AE, McDaniel TK, Donnenberg MS, Kaper JB (1995) Enteropathogenic Escherichia coli contains a putative type III secretion system necessary for the export of proteins involved in attaching and effacing lesion formation. Proc Natl Acad Sci USA 92:7996-8000.
6. Jerse AE, Yu J, Tall BD, Kaper JB (1990) A genetic locus of enteropathogenic Escherichia coli necessary for the production of attaching and effacing lesions on tissue culture cells. Proc Natl Acad Sci USA 87:7839-7843.
7. Deng W, Puente JL, Gruenheid S, Li Y, Vallance BA, Vazquez A, Barba J, Ibarra JA, O'Donnell P, Metalnikov P, Ashman K, Lee S, Goode D, Pawson T, Finlay BB (2004) Dissecting virulence: systematic and functional analyses of a pathogenicity island. Proc Natl Acad Sci USA 101:3597-3602.

8. Calderon Toledo C, Rogers TJ, Svensson M, Tati R, Fischer H, Svanborg C, Karpman D (2008) Shiga toxin-mediated disease in MyD88-deficient mice infected with Escherichia coli O157:H7. Am J Pathol 173:1428-1439.

Figure legends for supplementary figures

Figure 1. CD14 labeling in the human colon from Patient 1. CD14-positive cells (monocyte/macrophages) were demonstrated in the submucosa of the sigmoid colon from Patient 1 (**a**). The same area with TUNEL positive cells (**b**). Magnification x 200.

Figure 2. Intestinal pathology in inoculated mice. Distal (panels **a**,**b**,**c**,**f**) and proximal (panels **d**,**e**) colons from inoculated mice were stained using periodic acid Schiff and visualized by light microscopy. Infiltrates (arrows) were detected in the distal colons of mice infected with 86-24INT strain (**a**), CVD451$_{pCVD446}$INT strain (**b**) and UMD619FE strain (**c**). The inset in panel **a** shows vascular congestion in the same specimen. The inset in panel **b** shows mononuclear blood cells. Shrunken interstitial space was demonstrated in the proximal colon of a mouse inoculated with strain 87-23INT (**d**). The proximal (**e**) and distal colon (**f**) from a PBS control mice showed normal histology. Magnification x 100 (panels), x 400 (inset a), x 600 (inset b).

Figure 3. Inflammatory infiltrates in the distal colons of inoculated mice. Inflammatory infiltrates (defined as a group of six or more inflammatory cells) were quantified in the colonic tissues. The line inside each box represents the median. The upper and lower limits of the box-plot represent the interquartile range. The upper and lower limits represent the range. Outliers are marked with open circles. Significantly more infiltrates were found in the mice inoculated with strain 86-24INT compared to strain 87-23INT and PBS controls. * $P < 0,05$.

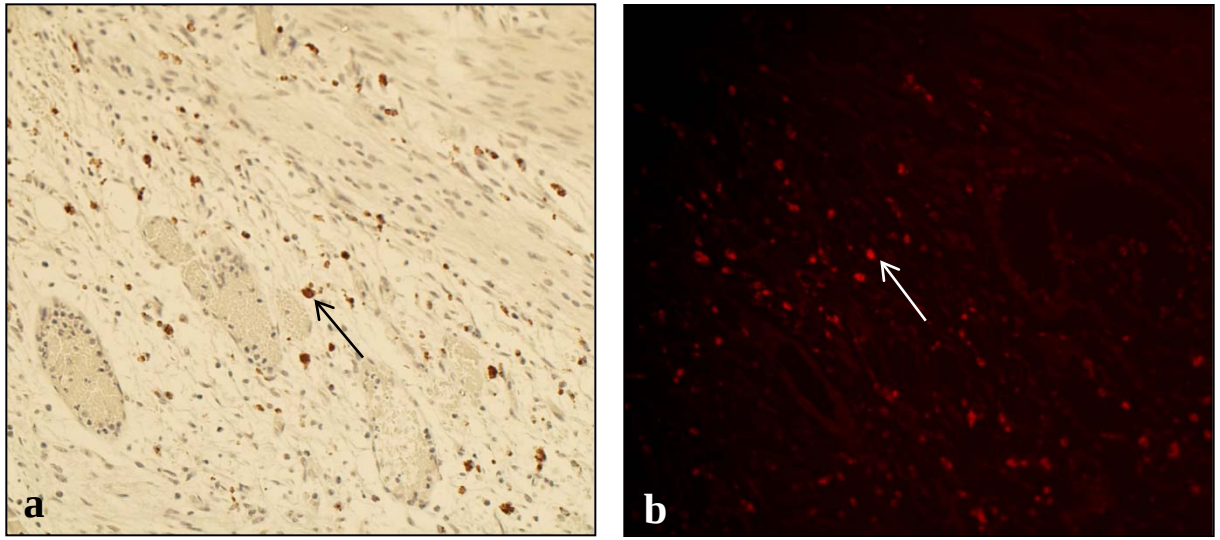

Figure S1

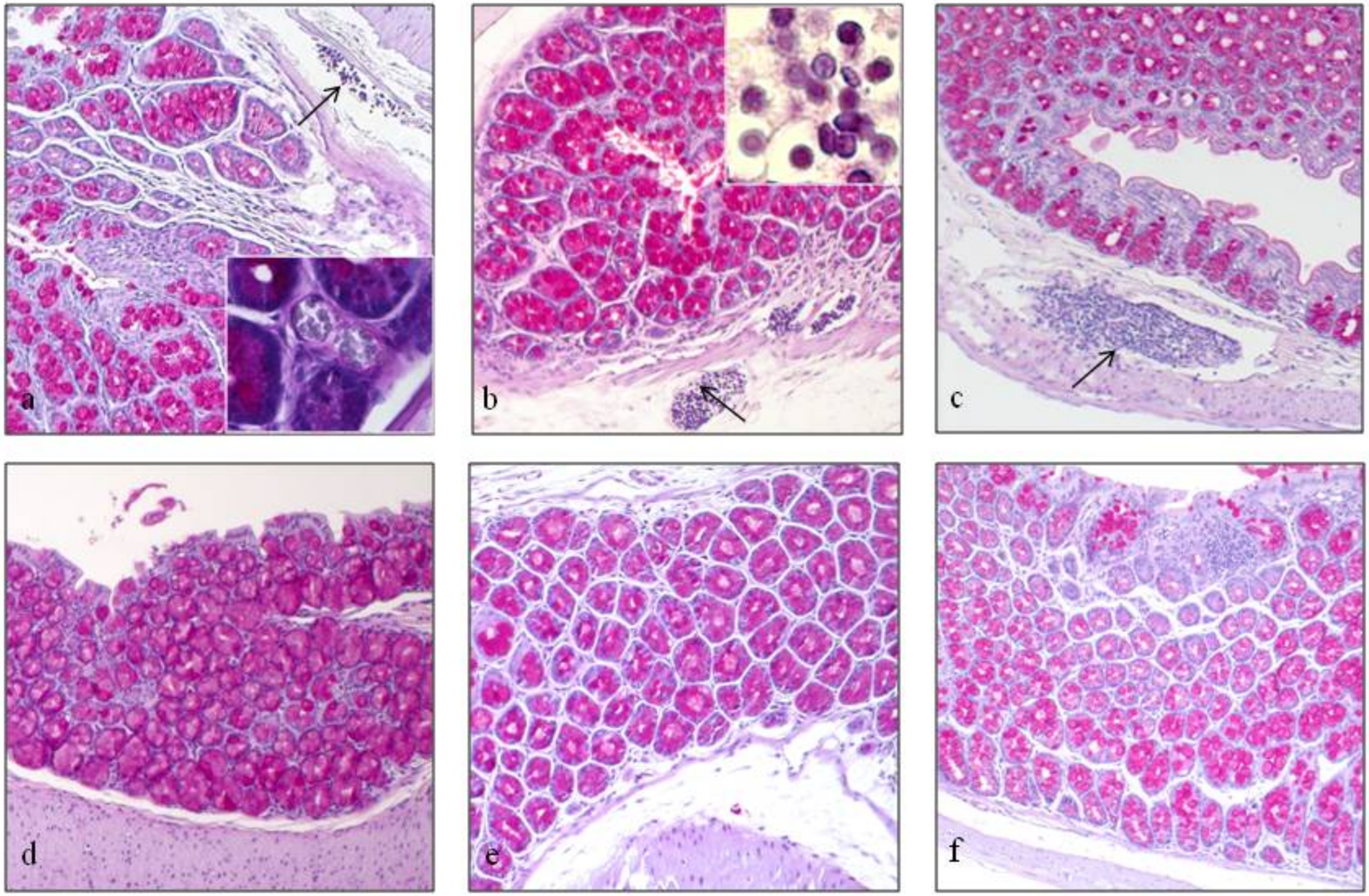

Figure S2

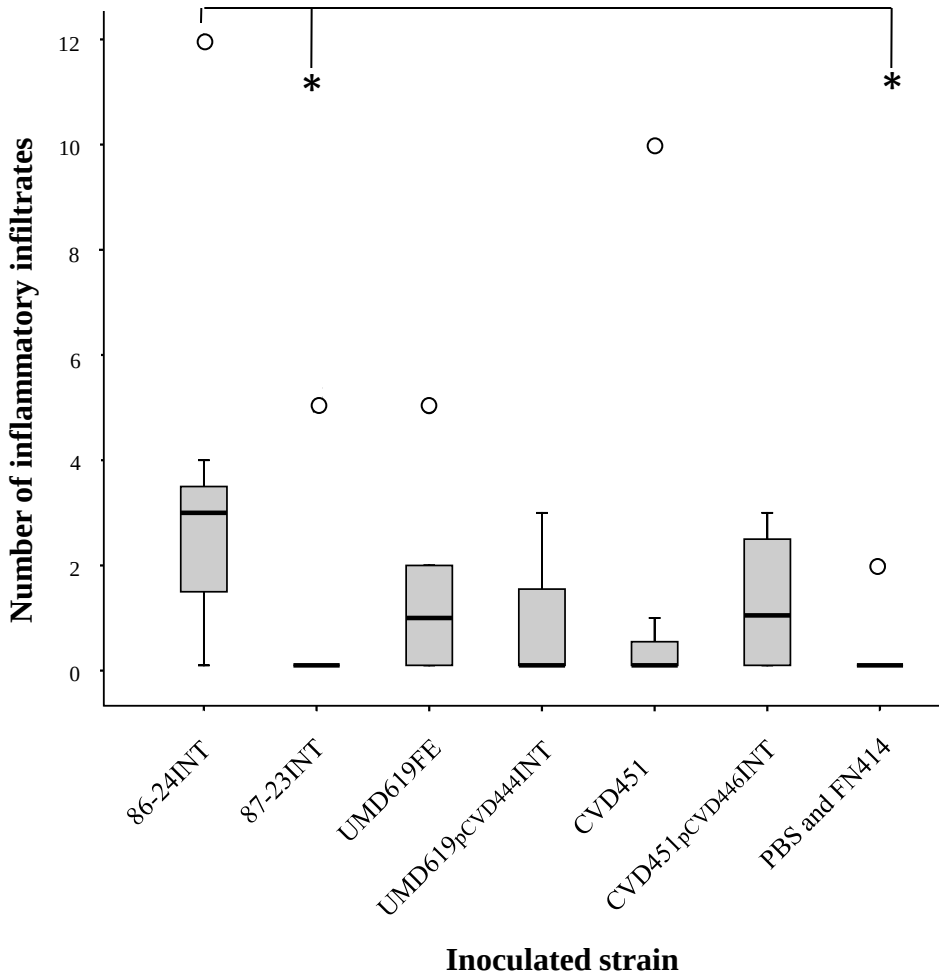
Number of inflammatory infiltrates
12
10
8
6
4
2
0
*
*
86-24INT
87-23INT
UMD619FE
UMD619pCVD444INT
CVD451
CVD451pCVD446INT
PBS and FN414
Inoculated strain

Figure S3